文章编号：0258-7025(2010)11-2703-06

# Hydration of Fingernail Investigated by Optical Coherence Tomography

Hao Zhang(张浩), Yaoyong Meng(孟耀勇)*, Wenjuan Ou(欧文娟), Xiaoyan Zhang(张小燕), and Songhao Liu(刘颂豪)

(*Photonic Chinese Medicine Laboratory, Institute of Biophotonics, South China Normal University, Guangdong, Guangzhou* 510631, *China*)

* *Corresponding author*: *mengyy@tom.com*

*Received May* 11, 2010; *Revised June* 14, 2010

**Abstract** Optical coherence tomography (OCT) is used to investigate the microstructure changes of human fingernail induced by hydration. Images of nail plate are obtained to display the morphology of fingernail and to disclose the keratinization of basal cells of nail plate. Combined with digital vernier caliper, this imaging technology is used to evaluate thicknesses and changes of nail *in vitro* after immersion with time. OCT images of nails show that the dorsal and ventral layers of nails have similar thicknesses which are much thinner than intermediate layer. The total thickness of fingernail exponentially increases with immersion time, and the saturating phenomenon appears at about 12 min. Three layers show different contributions to the total increase of the thickness of 17.4%. Microstructure changes *in vivo* are similar to the results *in vitro*. The changes of optical path length also could be evaluated by this method. OCT is capable of reflecting precise microstructure changes, and it has the potential to provide physician with a modern and objective diagnostic standard for nail inspection (NI) and to monitor disorders in Chinese traditional medicine (CTM) clinical practice and research.

**Key words** medical optics; optical coherence tomography; hydration; fingernail

**CLCN**: O433.4 **Document Code**: A **doi**: 10.3788/CJL20103711.2703

## 1 Introduction

Fingernail, which is a kind of human skin accessories, is composed of keratinized fibrin and keratin. It grows from nail root and matrix, and is supported by nail bed until it reaches nail free edge. The studies on composition and microstructure of fingernail have been previous reported. Olabanji *et al*. studied the elemental concentrations of fingernail to provide the evidence of skeletal elements by particle induced X-ray emission (PIXE)[1]. Caputo *et al*. investigated the freeze-fracture replicas of human nail plate to research the width of keratin filaments and the ultra structural differences between the modes of keratinization and the plasma membranes[2]. Farran *et al*. studied the relationship between microstructure and mechanical properties and revealed the functional morphology by scanning electrical microscopy[3]. Using the same technology, Forslind *et al*. found that the hard dorsal nail plate was supported by the plastic intermediate layer[4]. Piao *et al*. drew a conclusion that the harder intermediate layer was composed by the fibrous keratin, while the dorsal and ventral layers were the plate-like keratin[3~5]. However, due to the demands for the sample preparation and other related technologies, the above methods can hardly achieve *in vivo* and non-destructive detection.

Fingernail is very impervious and lowly penetrative to most of chemical agents. Vejnovic *et al*. researched the optimal permeation enhancers of drug deliveries through the nail plates to curve the fungal fingernail, and thought that hydrophobins were suggested efficient to be in drug delivery through the nail plate[6]. Water content plays an essential role in the keratinized tissues of fingernail. However, daily routines water touching impairs the keratin structure of nail, making it softer and more frangible. Finlay *et al*. used different ultrasound velocities to immersed fingernails and demonstrated changes of thickness[7,8]. Farran *et al*. evaluated the effects of humidity and mechanical properties,

This research was supported by the National Natural Science Foundation of China (60411130595) and the Program from Traditional Chinese Medicine Bureau of Guangdong Province (2008233).

and thought increasing relative humidity lowered the torsional stiffness, which plasticized the matrix rather than the fibers[3,9,10]. Barba *et al*. investigated the water content of fingernail keratinized tissues and concluded that the chemical treatments of nails impaired their integrity and led to a decrease in the internal water content. They researched the moisture absorption that showed a low regain and a much lower diffusion coefficient than human hair and made a conclusion that the diffusion coefficient was important in determining the integrity of keratin fibers[11]. Wessel *et al*. investigated the water uptake and saturating effect of nail samples after immersion and found that a saturating effect appeared after 10 min by near infrared Fourier transform Raman (NIR-FT-Raman) spectroscopy[12,13]. Marzec *et al*. found that the values of permittivity of dielectric spectroscopy with low content water showed significant differences, but three separate relaxations of permittivity and conductivity were similar for both healthy and diabetic nails [14].

Although this technology has been early applied to the ophthalmology[8], optical coherence tomography (OCT) is a recently developed and noninvasive imaging technique that provides high-resolution cross-sectional images of the microstructures of biological tissue[15, 16]. This technology is very popular and illustrates a good prospect of application and extension[17, 18]. It combines the advantages of interferometer and confocal microscopy to probe the weakly backscattered photons from the microstructures beneath tissue surfaces[19]. In this study, we observe the microstructure changes of fingernail *in vivo* before and after immersion to make a preparation for the study on nail inspective (NI) in Chinese traditional medicine (CTM) clinical practice and research.

## 2 Method

Nail fragments were collected from students and teachers of our laboratory ($n = 12$ *in vitro* and $n = 9$ *in vivo*). All donors had no obvious dermatopathic symptom and case history. Subjects kept fingernail clean and off water for at least 2 h before testing. Specimens of nail free edge were clipped when lengths of free edges were more than 5 mm and conserved in the dried and sealed ampules at room temperature before testing. Nail clippings were softly brushed and measured by the digital vernier caliper and OCT before and after being soaked in the double-distilled water at the 3-min interval from 0 to 30 min. Nail plates were examined *in vivo* from 9 volunteers after being soaked in water in the same interval from 0 to 15 min.

The OCT system is shown in Fig. 1. Imaging is obtained by directing low-coherence light to the sample and detecting the reflected ray from various internal structures by using an optical fiber integrated scanning system. A superluminescent diode with the central wavelength at 1310 nm and bandwidth of 50 nm was employed as the light source. The light was delivered via a single-mode fiber with a mode field diameter of 5.3 μm. A visible light source ($\lambda = 645$ nm) was used to guide the probe beam. The two-dimensional OCT images were obtained by scanning along $x$ and $y$ directions from dorsal and ventral surface of nail clippings, as shown in Fig. 1. Each in-depth scanning consisted of 10000 data points. The lateral scanning image was obtained by moving the mirror relative to the tissue sample. This system can provide an axial resolution of 10 ~ 15 μm and a transverse resolution of 15 ~ 25 μm. The signal-to-noise ratio (SNR) of this system was measured at 100 dB. The system was controlled automatically by computer and the control software was written in LabVIEW 7.2-D.

## 3 Results and Discussion

In the view of anatomy, nail plate origins from nail root, which is surrounded by nail matrix. Nail matrix is composed by the immature differentiated and formatted epithelial cells. These cells are polarized to prickle cells, which are further differentiated into hard orthokeratotic cells. These primary cells of different parts generate layers of nail plates. Basal cell divisions promote nail plate to grow forward free edge. The growing structure of nail plate was scanned by employing OCT. The shape of nail root was an oblique wedge. The nail root was surrounded by nail matrix, ventral position of which was considered the source of basal cells in Fig. 2(a). As basal cell proliferation, keratinocyte is pushed forwards with newly cell proliferation. Nail plate grows continuously. From Fig. 2 (b), it is seen that nail structure is relatively homogenous. Nail plate and dermis are separated by nail matrix. To the free edge shown in Fig. 2(c), nail plate starts to become off nail matrix, meanwhile the nail

matrix piles up and differentiates into stratum corneum. The growing structure permeates bio-life information and could provide a detailed statement about normal tissue to control pathological changes.

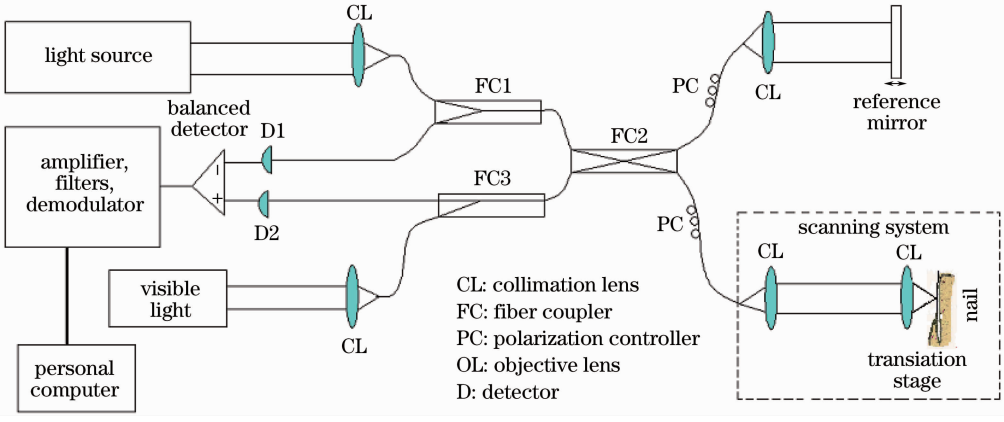


Fig. 1　Schematic of the OCT system.

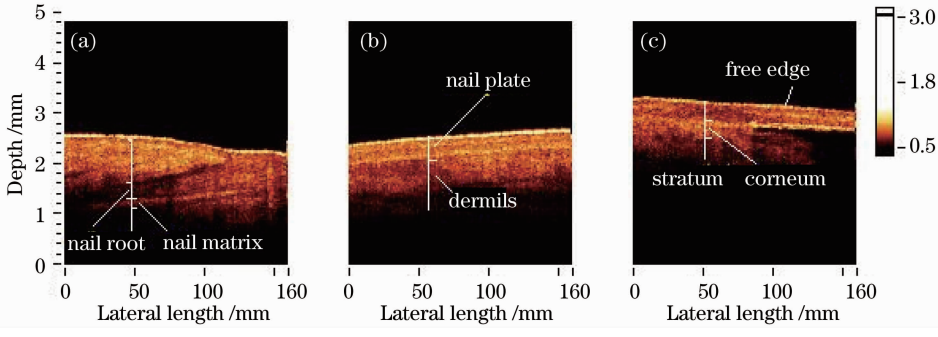


Fig. 2　OCT images of different locations of fingernail *in vivo*. (a) the nail root, (b) the middle part of fingernail, (c) the free edge of nail.

At the distal edge, free edge peels off nail matrix with nail plate growing. Free edge corresponds to nail plate, which is made up of hard keratinocyte cells. The arrangements of these cells construct the structures of three nail layers that have been detected by some physical methods[5,19,20]. The two-dimensional OCT image is obtained along the surface of fingernail clipping. The three-layer structure from OCT image is consistent with the previous researches[21], as shown in Fig. 3(a). Micro-structure is visible because of arrangemental modes of keratins. The dorsal and ventral layers appear to be composed of flat, overlapping slate-like sheets. In contrast, the intermediate layer is more fibrous and parallel to the free edge of fingernail. The gray values with depth of low-interference show clearer differences among three layers. There are two conspicuous dark marks next to the dorsal and ventral internal surfaces. The marks are the boundaries between dorsal layer and intermediate layer and be-

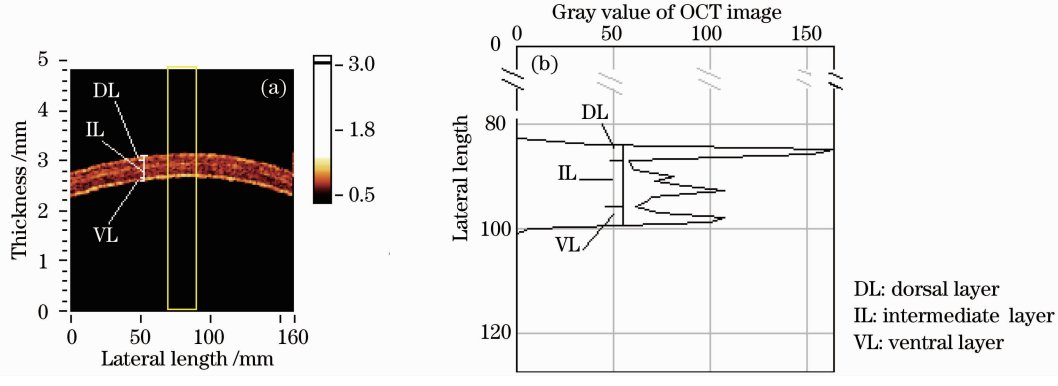


Fig. 3　(a) OCT image of fingernail clipping surface structure, (b) distribution of the gray value of the OCT image along the interference depth, corresponding to the rectangle in (a).

tween ventral layer and intermediate layer. The values were calculated from chippings of fingernail by OCT and processed by the software of Origin7.5 in Fig.4. The time-dependent charts show the depth of the dorsal, intermediate, and ventral layer, respectively. Human fingernail plate is one of the most impervious biological structures, and the penetration of chemical agents is low[14]. However, water is apt to influence nail keratin. Being saturated in double-distilled water, the total thickness of fingernail increases, as can be seen from Fig.4(d). Hydration is thought to be the most important factor influencing the physical properties of nails and possibly acts through changes in keratin structure[21]. However, three layers discriminate in trends of thickness changes from the OCT images, as shown in Figs.4(a)～(c). Nail plate increases by 17.4% after immersion. This indicates that nail has a definite water holding capacity. Three layers of nail plates have different contributions to the total thickening. The dorsal and ventral layers increase by 22.9% and 28.2%, respectively, while the intermediate layer increases by 14.6%. Though the increasing degrees of the formers two layers are higher than the latter, the intermediate layer has the more support. During time interval from 9 to 12 min, the thickness of nail plate increases to the maxima due to the saturation[22]. Although the dorsal and ventral layers have higher rates, they show less contribution to the total change of fingernail plate because of the keratin arrangement. The intermediate layers have the actual thickness to mainly protect the nail. Hydration makes the fingernail softer and more frangible.

The change trend of thickness in immersion is exponential. These data further document the changes of fingernail after immersion. The related parameters, coefficients, and function are given in Table 1.

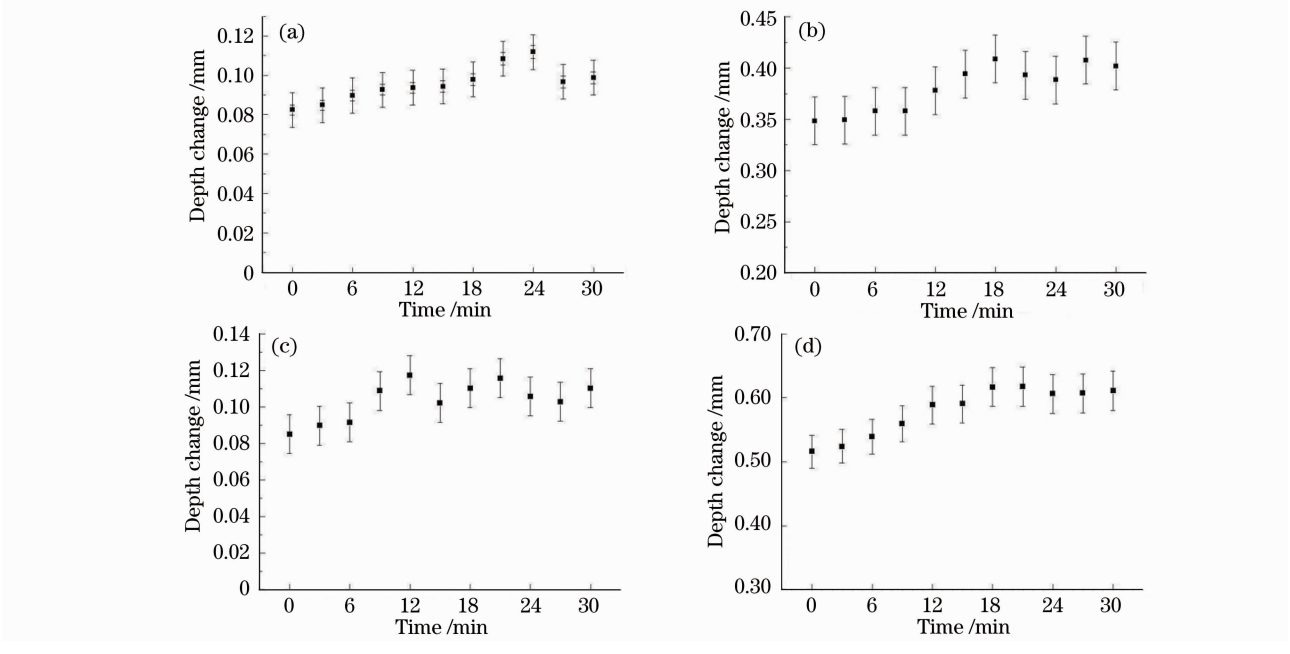


Fig.4 Time-dependent changes of three layers thicknesses and total depth during the immersion: the time interval is 3 min. (a), (b), (c), and (d) show the changes of the dorsal, intermediate, ventral, and total layer depths, respectively.

Table 1 Fit equation and parameters of the change of fingernail saturated in water

| The fit function | $Y = Y_0 + A_1\exp(-x/T_1)$ | | |
|---|---|---|---|
| | $Y_0$ | $A_1$ | $T_1$ |
| The dorsal layer | 0.098 | −0.046 | −2.460 |
| The intermediate layer | 0.243 | −0.022 | 2.153 |
| The ventral layer | 0.105 | −0.020 | 2.702 |
| The total depth measured by OCT | 0.543 | −0.057 | 1.744 |
| The total depth measured by digital vernier caliper | 0.547 | −0.057 | 1.752 |

OCT images appeared to be similar before and after immersion. Nail matrix is a bifacial boundary which conglutinates between nail plate and nail bed. After immersion, the nail matrix has relatively lower gray value and the nail plate is more clearly divided from the nail bed. The nail plate apparently becomes thicker by comparing Figs. 5(a) with (c). For a fine detail, the curves of gray value is different with that before immersion, as can be seen from Figs. 5(b) and (d). At the interface between air and nail plate, gray value is lower after immersion. The distribution of gray value of the nail plate is comparatively uniform, and the gray value of the nail matrix decreases rapidly with less fluctuation. This difference appears due to the interaction between water and keratin. As a vector for the complex treatment, water could change the microenvironment to help pharmaceutical ingredients to the focus of infection of fingernail. Meanwhile, OCT was used as a tool for measuring the thickness changes of nail plate *in vivo* after immersion. Its thickness increased by 14.8%. This extremely tallied with the result *in vitro*.

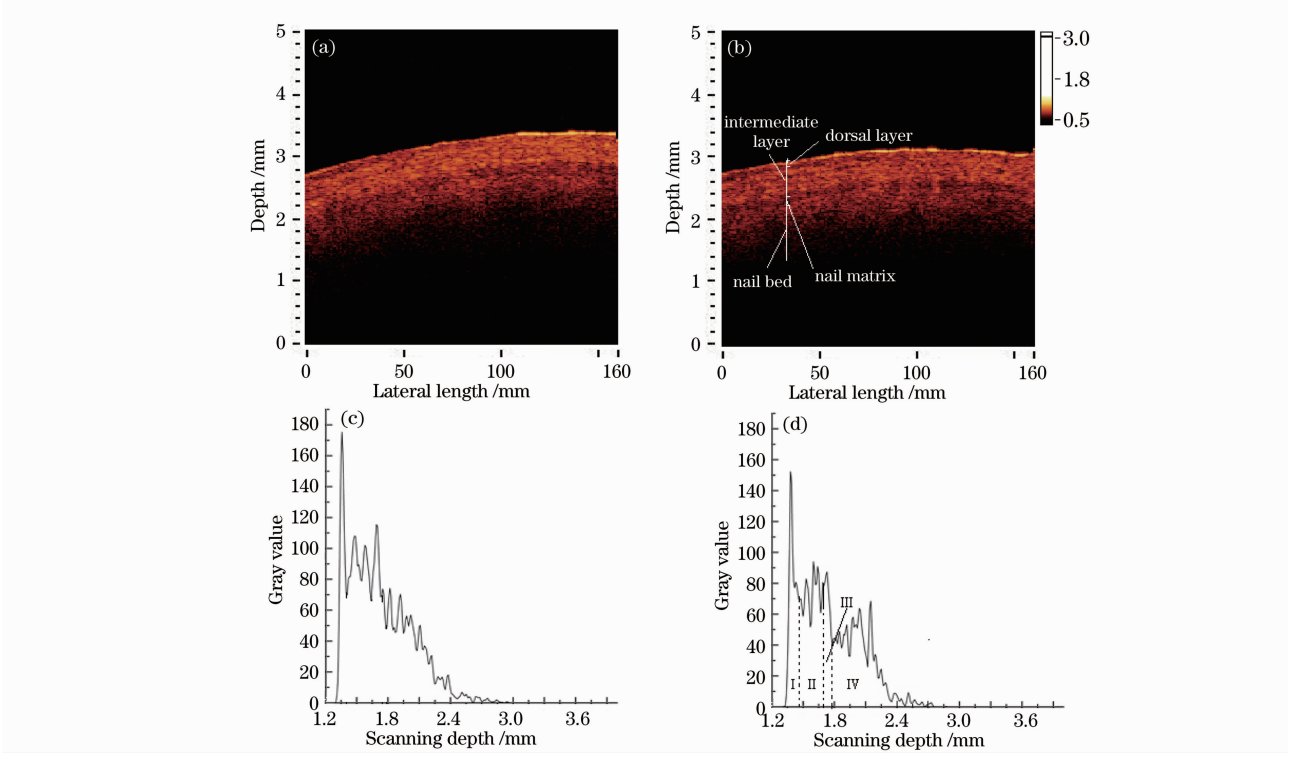


Fig. 5　OCT images of fingernail *in vivo* (a) before and (b) after immersion and (c), (d) the corresponding gray value distributions Ⅰ, Ⅱ, Ⅲ, and Ⅳ correspond to the dorsal layer, the intermediate layer, the nail matrix, and the nail bed, respectively.

Refraction index of biological tissue is a basic parameter that characterizes how light interacts with biological tissue. However, refraction index is different according to the permittivity of tissues, which is related to the density of tissue and changes if the tissue is affected by other materials. Due to keratin structures, the depth changes of three layers are different. When optical distance is measured by using OCT, the optical path length ($\Delta$) defined as the real path length ($\mathrm{d}l$) multiplied by the refractive index ($\mathrm{d}n$) of the medium in which the light is propagating is obtained: $\Delta = \mathrm{d}l \times \mathrm{d}n$. Because $\mathrm{d}n$ is related to the number of atoms per unit volume, $\Delta$ changes after immersion, and shows different tendencies according to the microstructures of three layers.

## 4　Conclusion

We have demonstrated the time-dependent changes of the properties of fingernail structure influenced by water *in vitro* using OCT. The combination of water and keratins leads to the changes of properties of fingernail. OCT, which is suitable to display the time-dependent changes of the physical properties of fingernail, is a noninvasive imaging technique that provides the high-resolution cross-sectional images of the microstructures of biological tissue. It is capable of sensitive-

ly monitoring the change of fingernail in intermission. OCT has a potential to be developed into a useful tool for NI in CTM clinical practice and diagnostic. So, using OCT to trace the progress of treatment of nail disorder *in vivo* is very significant and potential.

## References


1 S. O. Olabanji, O. A. Ajose, N. O. Makinde *et al*.. Characterization of human fingernail elements using PIXE technique[J]. *Nuclear Instruments and Methods in Physics Research B*, 2005, **240**(4): 895～907

2 R. Caputo, G. Gasparini, D. Contini. A freeze-fracture study of the human nail plate[J]. *Archives of Dermatological Research*, 1982, **272**(1-2): 117～125

3 L. Farran, S. Eichhorn, R. Ennos. The microstructure and mechanical properties of human fingernail [J]. *Comparative Biochemistry and Physiology, Part A*, 2007, **146**(4): S107～S127

4 B. Forslind, N. Thyresson. On the structure of the normal nail[J]. *Archives of Dermatological Research*, 1975, **251**(3): 199～204

5 Daqing Piao, Doug Abreski, Quing Zhu. Preliminary results of imaging and diagnosis of nail fungal infection with optical coherence tomography[C]. Technical Digest of OSA Biomedical Topical Meetings, 2002. 65～68

6 Ivana Vejnovic, Linda Simmler, Gabriele Betz. Investigation of different formulations for drug delivery through the nail plate[J]. *International J. Pharmaceutics*, 2010, **386**(1-2): 185～194

7 A. V. Finlay, P. Frost, A, D. Keith *et al*.. An assessment of factors influencing flexibility of human fingernails[J]. *British J. Dermatology*, 1980, **103**(4): 357～365

8 A. Finlay, B. Western, C. Edwards. Ultrasound velocity in human fingernail and effects of hydration: validation of in vivo nail thickness measurement techniques[J]. *British J. Dermatology*, 1990, **123**(3): 365～373

9 L. Farran, A. R. Ennos, M. Starkie *et al*.. Tensile and shear properties of fingernails as a function of a changing humidity environment[J]. *J. Biomechanics*, 2009, **42**(9): 1230～1235

10 L. Farren, S. Shayler, A. R. Ennos. The fracture properties and mechanical design of human fingernail[J]. *The J. Experimental Biology*, 2004, **207**(5): 735～741

11 C. Barba, M. Martí, A. M. Manich *et al*.. Water absorption/desorption of human hair and nails[J]. *Thermochimica Acta*, 2010, **503-504**: 33～39

12 Sonja Wessel, Monika Gniadecka, Gregor B. E. Jemec *et al*.. Hydration of human nails investigated by NIR-FT-Raman spectroscopy[J]. *Biochemical et Biophysics Acta*, 1999, **1433**(1-2): 210～216

13 J. Welzel. Optical coherence tomography in dermatology: a review[J]. *Skin Research and Technology*, 2001, **7**(1): 1～9

14 E. Marzec, J. Olszewski. Molecular interactions in human nail plate analysed by dielectric spectroscopy [J]. *Colloids and Surfaces B: Biointerfaces*, 2009, **69**(1): 91～94

15 Li Peng, Huang Run, Gao Wanrong. Experiment research on optical coherence tomography of human skin [J]. *Chinese J. Lasers*, 2009, **36**(10): 2498～2502
李 鹏, 黄 润, 高万荣. 光学相干层析术在人体皮肤成像方面的实验研究[J]. 中国激光, 2009, **36**(10): 2498～2502

16 Duan Lian, He Yonghong, Zhu Rui *et al*.. Development of a spectrum domain 3D optical coherence tomography system[J]. *Chinese J. Lasers*, 2009, **36**(10): 2528～2533
段 炼, 何永红, 朱 锐 等. 三维谱域光学相干层析成像系统的研制[J]. 中国激光, 2009, **36**(10): 2528～2533

17 Yang Yaliang, Ding Zhihua, Meng Jie *et al*.. Common path optical coherence tomography system suitable for endoscopic imaging[J]. *Acta Optica Sinica*, 2008, **28**(5): 955～959
杨亚良, 丁志华, 孟 婕 等. 适合于内窥成像的共路型光学相干层析成像系统[J]. 光学学报, 2008, **28**(5): 955～959

18 He Yongjian, Gao Yingjun, Li Kui *et al*.. Optical coherence tomography images processing[J]. *Acta Photonica Sinica*, 2009, **38**(6): 1464～1468
何永建, 高应俊, 李 逵 等. 光学相干层析图像的处理研究[J]. 光子学报, 2009, **38**(6): 1464～1468

19 Shi Guohua, Ding Zhihua, Dai Yun *et al*.. Ophthalmic imaging by optical coherence tomography [J]. *Chinese J. Lasers*, 2008, **35**(9): 1429～1431
史国华, 丁志华, 戴 云 等. 光纤型光学相干层析技术系统的眼科成像[J]. 中国激光, 2008, **35**(9): 1429～1431

20 Haixin Dong, Zhouyi Guo, Chengchun Zeng *et al*.. Quantitative analysis on tongue inspection in traditional Chinese medicine using optical coherence tomography[J]. *J. Biomedical Optics*, 2008, **13**(1): 011004

21 D. C. Pope, W. T. Olive. Dimethyl Sulfoxide (DMSO)[J]. *Can. J. Comp. Med. Vet. Sci.*, 1966, **30**(1): 3～8

22 H. Bharadwaj, M. V. Singh, S. B. Rawal *et al*.. Hydration and tissue solid content of the lean body on prolonged exposure to altitude[J]. *International J. Biometeorology*, 1989, **33**(1): 27～31